JOURNAL OF MATERIALS SCIENCE 30 (1995) 6257–6266

Mechanical stability and magnetic properties of austenite

M. AHMED, I. NASIM, H. AYUB, F. H. HASHMI, A. Q. KHAN
Dr A. Q. Khan Research Laboratories, Kahuta, Pakistan

Austenitic alloys have been produced by additional alloying in maraging steel grade 18 Ni at 2400 MPa. The concentration of Mo, Ni and Co was increased individually until the martensite start temperature M_s, was suppressed below ambient value. Charpy impact strength, tensile strength and magnetic properties were determined. The impact strength in the annealed condition ranged between 260 to 294 J. In alloys where martensitic transformation occurred following quenching in liquid nitrogen, the impact strength dropped appreciably and was found to be in the range 120–216 J. The tensile strengths of the austenite and martensite phases ranged between 680 to 890 and 1030 to 1100 MPa, respectively. It was observed that the austenite phase transformed to martensite in the region that under went plastic deformation during Charpy and tensile testing. The degree of transformation incorporated, varied as a function of composition. The magnetic properties of the austenite phases were typical of a very weak magnetic material. The coercive field and saturation magnetization values were in the range 1034–2387 $A m^{-1}$ and 1.6–2.9 T, respectively. In contrast to the general observation, the austenite phase containing high Co exhibited ferromagnetic behaviour. The coercive field and saturation magnetization of ferromagnetic austenite was 1034 $A m^{-1}$ and 11 T, respectively.

1. Introduction

The present work examines a unique group of austenite alloys developed as a consequence of research on ultra high strength maraging steels [1]. The starting material, in which additional alloying was carried out to produce modified compositions, was comprised of the conventional 18 Ni–2400 MPa grade maraging steel. The composition of Mo, Ni and Co was increased, one at a time, while other elements were kept at a level maintained in the conventional 18 Ni–2400 MPa grade. It was found that when the concentration of either of the three elements, i.e. Mo, Ni and Co, was increased to 7.5, 24 and 25 wt %, respectively, the austenite phase became stable up to ambient temperature.

The mechanical stability of these alloys was investigated following cold rolling to different degrees of reduction. The thermal stability was checked by dipping in liquid nitrogen. The Charpy impact and tensile strength were determined in the annealed condition and following quenching in liquid nitrogen.

In certain applications the magnetic properties of the austenite phase can also be of interest. Contrary to popular understanding that the austenite phase is paramagnetic, it was observed that high Co containing austenite exhibited ferromagnetic behaviour.

2. Experimental procedure

The chemical composition of the starting material and the alloys produced is given in Table I.

Melting and casting were carried out in a vacuum induction melting and casting furnace. High purity elements were used for additional alloying purposes. The ingots, weighing 12 kg, were forged after soaking at 1250 °C for 3 h. The final product was in the form of square and round bars of 14 × 14 mm sides and 14 mm diameter, respectively. The details regarding melting and forging have been presented elsewhere [2]. In order to study the mechanical stability of austenite, small pieces from the forged rods were cut and rolled in a laboratory scale rolling mill. The reduction ratio

TABLE I Composition of the alloys investigated (in wt %)

	18 Ni–2400 MPa steel	Alloy 1	Alloy 2	Alloy 3	Alloy 4
Ni	18.10	18.50	24.20	18.50	24.00
Co	12.20	11.50	11.50	24.00	11.00
Mo	3.80	7.50	3.50	3.60	7.50
Ti	1.70	1.50	1.50	1.60	1.50
Al	0.08	0.11	0.10	0.12	0.08
C	0.02	0.03	0.02	0.02	0.02
Fe	Balance	Balance	Balance	Balance	Balance

0022–2461

was varied between 50 to 90%. The magnetic properties were determined using Riken Denshi BHV 3.5 series vibrating sample magnetometer. The important instrument parameters and other variables used in magnetic measurements have been described elsewhere [3]. Magnetic properties were determined, at room temperature, in the as-rolled condition (~90% reduction), following annealing at 850 °C for 1 h in a vacuum furnace and after dipping the annealed material in liquid nitrogen (the dipping time was fixed at 15 min unless mentioned otherwise). The tensile and Charpy impact tests were carried out in the annealed condition and also after dipping in liquid nitrogen. Standard specimens were machined from the forged rods as per ASTM specifications. As in the case of magnetic properties measurement, the specimens

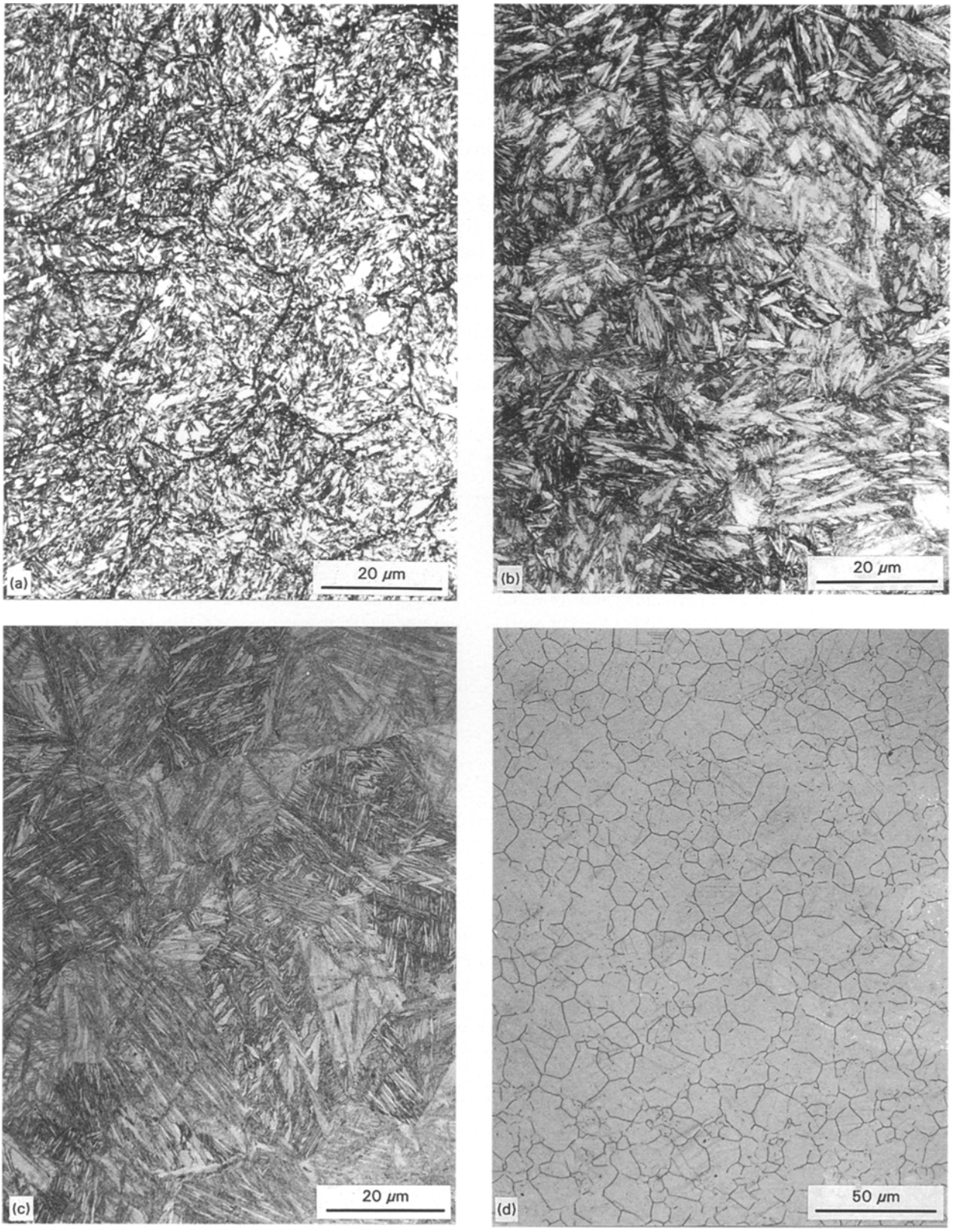

Figure 1 Microstructure observed after dipping in liquid nitrogen for 1 min: (a), (b), (c) and (d) represent optical images obtained from alloys 1, 2, 3 and 4, respectively.

after dipping were brought back to room temperature before testing. The austenite to martensite transformation was monitored using an X-ray diffraction technique. The direct comparison method of Averback and Cohen was used [4]. In the case of the cold rolled specimens, the appropriate peaks, that give representative results were used [5]. The vol % austenite transformed during tensile testing was determined in the deformed region of the tensile specimen. Hardness was measured as a function of distance from the fractured edge. The length of the specimen that exhibited more or less uniform hardness was cut off (these lengths were of the order of 10 mm). Thin slices were cut from this piece using a diamond blade and were cold mounted and polished before X-ray analysis. In case of Charpy specimens, slices were machined off from the area just below the fracture surface. However, inherent to the tests, the deformed region, because of the notch and the high strain rate, was limited and only qualitative analysis could be carried out. Scanning electron microscopy (SEM) was used to study fractured surfaces.

3. Results and discussions

Both Mo and Ni are known to be austenite stabilizers and their presence beyond a certain critical level shifts the M_s temperature below the ambient value. The critical concentration of Mo and Ni was found to be 7.5 and 24 wt %, respectively [1]. The suppression of M_s temperature in Co added alloy was unexpected. When the Co content was increased to ~25 wt %, the austenite phase became stable. A highly stable austenite phase was observed when Ni and Mo were added together. The composition of the alloys investigated has been presented in Table I.

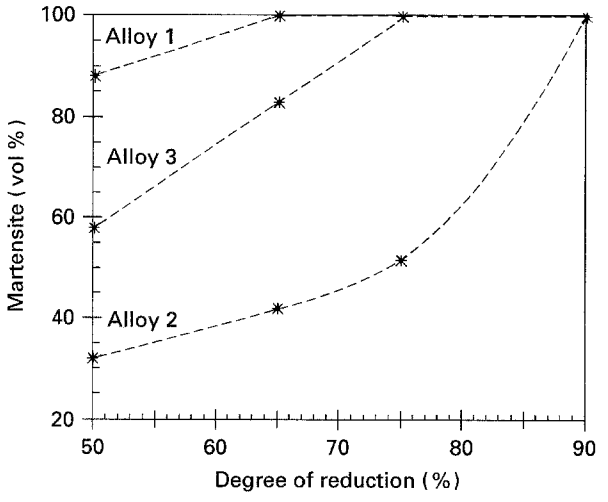

Figure 2 Vol % transformed martensite plotted as a function of reduction ratio.

All the alloys, with the exception of alloy 4, transformed to martensite when dipped in liquid nitrogen. Alloy 4 remained austenitic regardless of the quenching time. Fig. 1 depicts the microstructures observed after dipping in liquid nitrogen for 1 min. Well defined martensitic platelets are present in all the alloys, while equiaxed grains of the austenite phase are visible in alloy 4 (the size of the martensite platelets decreases as the quenching time increases [1]). The transformation to martensite also occurred when the alloys were cold rolled. The vol % martensite formed as a function of reduction ratio is presented in Fig. 2. As is clear from the figure, reduction ratios needed to induce complete transformation in alloy 1, alloy 2 and alloy 3 were ~65, ~90 and ~75%, respectively. Alloy 4 remained face centred cubic regardless of the degree of reduction employed.

One of the most remarkable features of the austenitic alloys investigated was their ultra high toughness. The Charpy impact values observed in the annealed condition and also following liquid nitrogen quenching are presented in Table II. The corresponding hardness values are also included in the table.

The fractured surfaces were examined in a scanning electron microscope. The fractographs obtained from alloy 1 in annealed and following liquid nitrogen quenching are depicted in Fig. 3. The fracture surfaces are typical of highly ductile material. The low magnification images obtained from the austenite and the martensite phase show that the shear dimples in the annealed material are relatively more elongated, see Fig. 3a, b, respectively. In the annealed material, a band type of distribution, where large dimples are separated by relatively smaller ones, can also be seen. In the case of martensite, however, the dimples are relatively more uniform in size and shape. The higher magnification images presented in Fig. 3c, d also indicate that the number density of dimples in the face centred cubic alloy is lower compared to the body centred cubic phase. Images obtained from alloy 3 in the annealed state and following liquid nitrogen quenching are presented in Fig. 4. In contrast to alloy 1, the band type of feature is present in both cases, Fig. 4a, b, respectively. The dimples in the annealed case are much more elongated compared to the liquid nitrogen dipped specimens. At higher magnification, the presence of a band type distribution

TABLE II Charpy impact strength of the austenite and martensite phases

Alloy	Austenite		Martensite	
	Impact toughness[a], J	Hardness[a], H_V	Impact toughness[a], J	Hardness[a], H_V
Alloy 1	290	220	216	390
Alloy 2	260	160	120	325
Alloy 3	294	210	186	310
Alloy 4	290	180	–	–

[a] The values represent an average of four readings. The error in impact and hardness values was ± 6 and $\pm 5 H_V$, respectively.

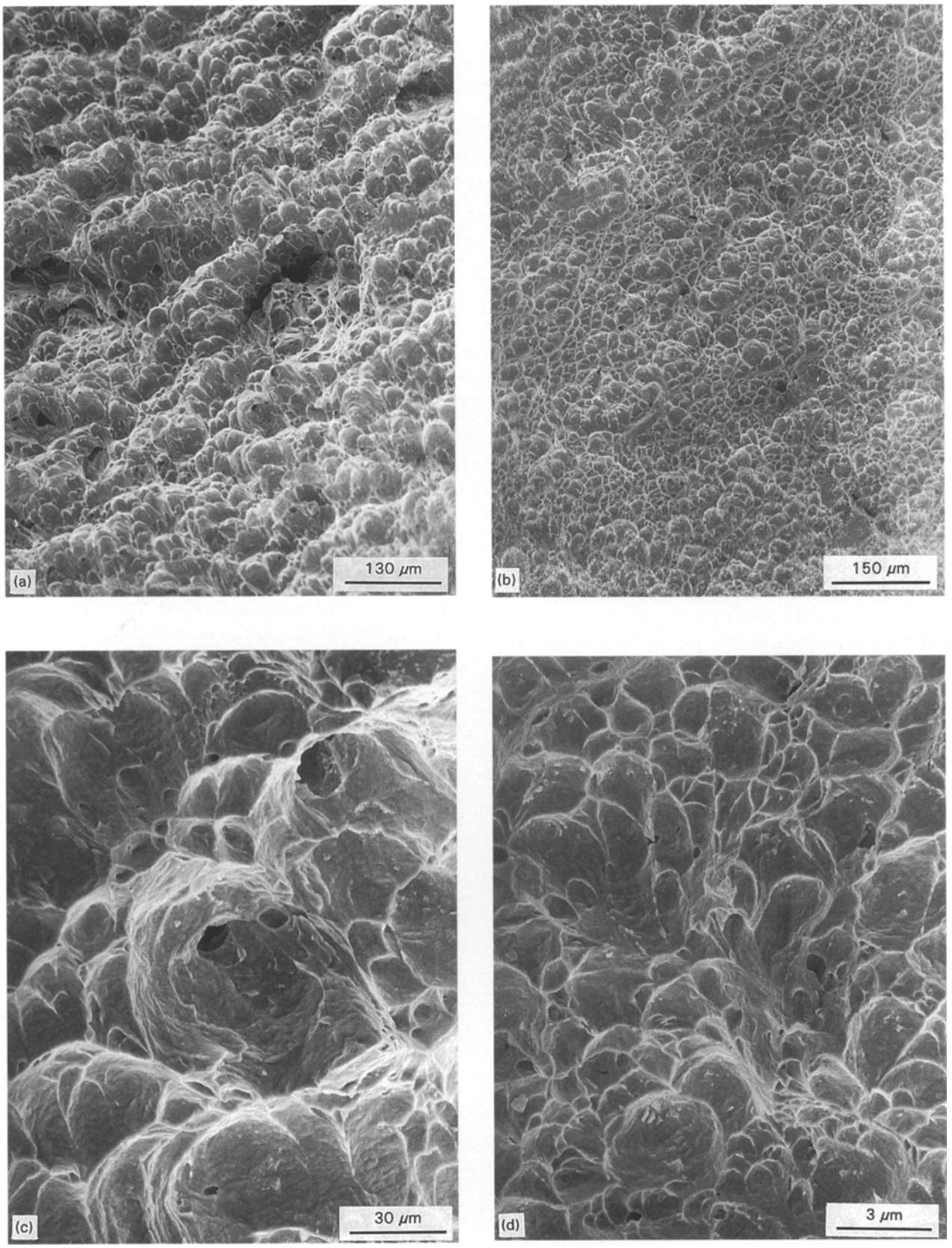

Figure 3 SEM fractographs obtained from alloy 1: (a) and (c) in the annealed condition, (b) and (d) following quenching in liquid nitrogen.

is more clearly defined in the annealed material compared to the dipped one, Fig. 4c, d, respectively.

A sharp difference in the appearance of the fracture surface was observed in the case of alloy 4. Images of the fractured surface obtained at different magnifications are presented in Fig. 5. The fracture surfaces were devoid of dimples, Fig. 5a. The image presented in Fig. 5b shows some evidence of shallow, elongated shear dimples, but most of the area remains dimple free. At higher magnification, the surface appeared heavily smeared, Fig. 5c. In some regions of the fractured surface, fine slip lines were also visible, Fig. 5d.

As mentioned earlier, the annealed material when subjected to cold rolling transforms to martensite. Similar transformation is expected in the plastically deformed region of the impact specimen. X-ray

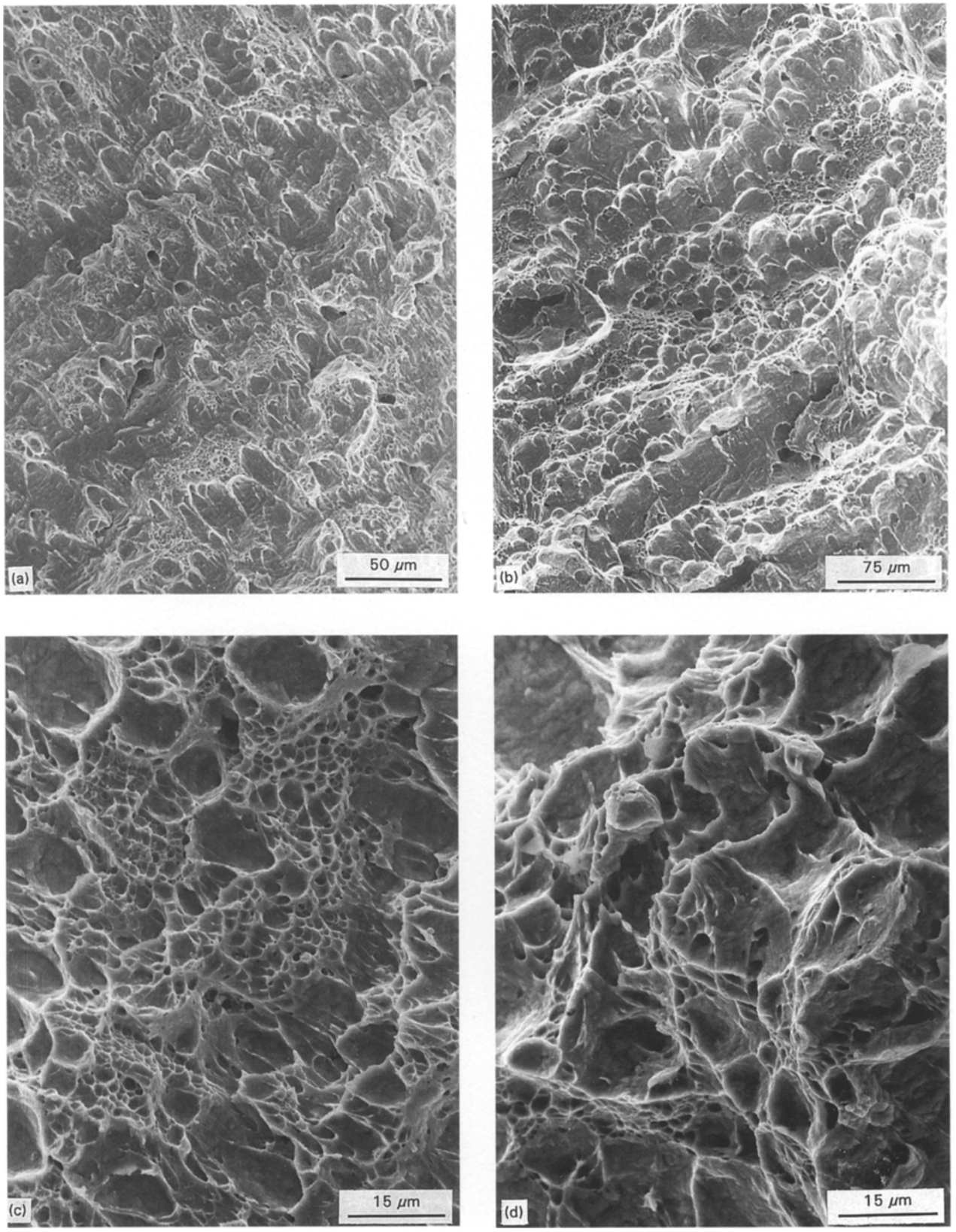

Figure 4 SEM fractographs obtained from alloy 3: (a) and (c) in the annealed state, (b) and (d) after dipping in liquid nitrogen.

analysis carried out on slices machined off from volume below the fractured surface show martensite peaks in addition to those expected of the austenite phase. The band structure, comprised of large and small dimples, observed in the annealed specimen may in some way be related to the transformation from the face to the body centred cubic phase during plastic flow. The large dimples may have formed in the face centred cubic region, whereas the smaller ones may have resulted following transformation to the body centred cubic phase. This, at present, is only a speculation and more work is needed to prove the same. The X-ray analysis carried out on the plastically deformed material of Charpy tested alloy 4 showed that the material remained face centred cubic. The fracture behaviour obtained in alloy 4, therefore, represents material failure in a highly stable face centred cubic alloy possessing very high impact strength.

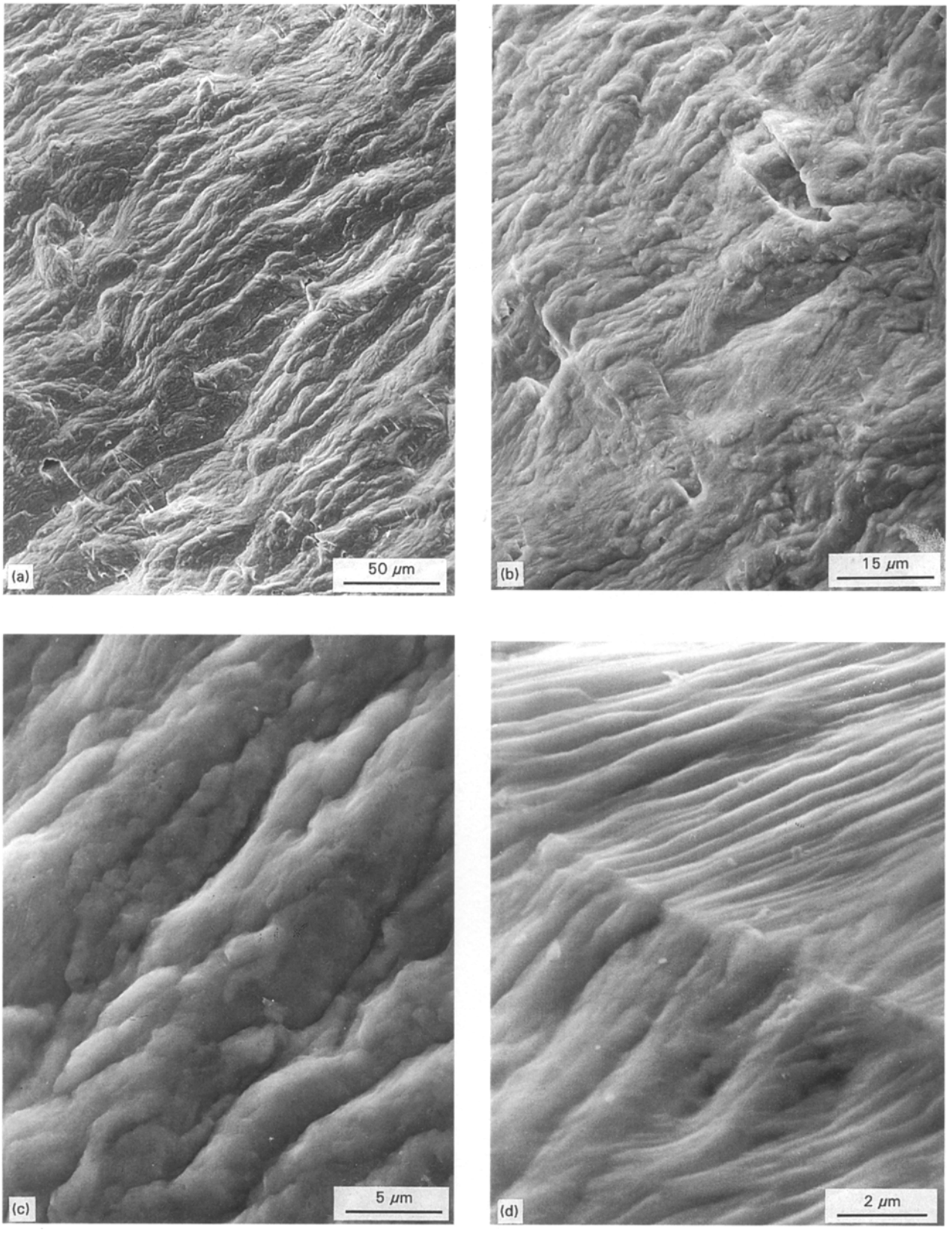

Figure 5 SEM images obtained from fractured surfaces in alloy 4: (a), (b) and (c) represent images at different magnifications; (d) high magnification image showing slip lines.

The tensile strength of the alloys was measured in the annealed state and following dipping in liquid nitrogen. The engineering stress–strain curve of alloy 3 is depicted in Fig. 6. The difference in the annealed and liquid nitrogen dipped curve represents the behaviour of the face and body centred cubic material when subjected to load under uniaxial tension. The austenite, as expected of a face centred cubic material, yields at a lower stress level in comparison to the martensite. The ratio between ultimate (UTS) and yield strength is much higher in case of the face centred cubic material, signifying a greater degree of work hardening during material flow. The data obtained for all the alloys is presented in Table III.

The alloys exhibited substantial increase in hardness and strength following martensitic transformation.

The only exception was alloy 4 where very little change was seen. The average hardness of the deformed region is also presented in Table III. These values were determined in the region that had undergone plastic flow during tensile testing.

The increase in hardness observed in the deformed region was due to cold work incorporated and, in the case of the annealed material, the added hardness due to phase transformation from austenite to martensite. The X-ray spectra from the deformed region of the tensile specimen in alloys 2 and 4 are depicted in Fig. 7. Spectra from alloy 2 exhibited peaks coming mainly from the transformed martensite phase. In contrast, the X-ray spectra from alloy 4 showed that the material remained face centred cubic during and after tensile testing. (The spectra from alloys 1 and 3 were similar to the one presented in Fig. 7a.) The vol % of the transformed martensite is also presented in Table III. It is interesting to note that the per cent elongation in alloys 1, 2 and 3 is higher compared with alloy 4. It is quite possible that the transformation from face to body centred cubic forms during plastic flow helps in accommodating some of the strain.

The fractographs obtained in alloy 3 after tensile testing in the annealed state and after dipping in liquid nitrogen are presented in Fig. 8. Well defined deep equiaxed coarse and fine dimples are visible in the primary fracture area, Fig. 8a, b, respectively. In both cases the large dimples are surrounded by a network of fine dimples. Surfaces within the dimples exhibit features that have developed due to plastic flow. In the shear lip area, very fine shear dimples can be seen in both the annealed and dipped cases, Fig. 8c, d, respectively. The similarity between the fracture surfaces of face and body centred cubic material can perhaps be related to the fact that the austenite transforms to martensite before rupture finally occurs.

In alloy 4 the martensitic transformation does not occur regardless of the treatment imparted. A low magnification fractograph, obtained from the primary fracture surface, is shown in Fig. 9a. Both large and small dimples are visible. A higher magnification image exhibits features within the dimples that resemble serpentine glide and ripples, Fig. 9b. The image obtained from the shear lip region is presented in Fig. 9c. The surface is heavily smeared and devoid of dimples. There is a sharp resemblance between the fractograph obtained from the shear lip area of the tensile specimen and the fracture surface obtained in the Charpy test. The resemblance of the two surfaces shows that when alloy 4 is fractured in a shear mode, the conventional dimples are not seen, instead a heavily smeared surface is obtained.

The magnetic properties of the austenite phases were determined in the annealed condition, after dipping the same annealed specimens in liquid nitrogen

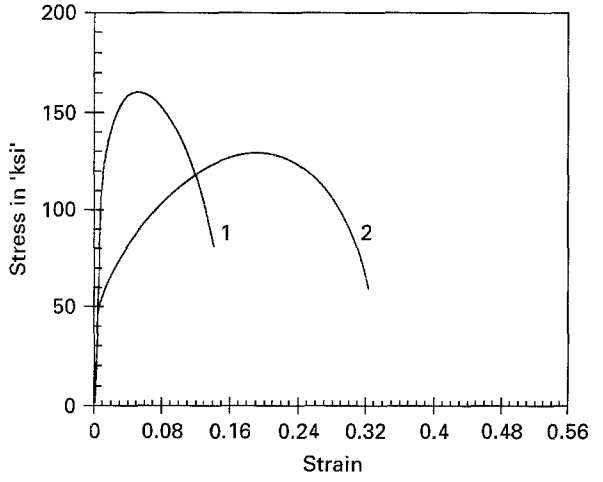

Figure 6 Engineering stress–strain curve of alloy 3 in annealed condition (2) and after dipping in liquid nitrogen (1).

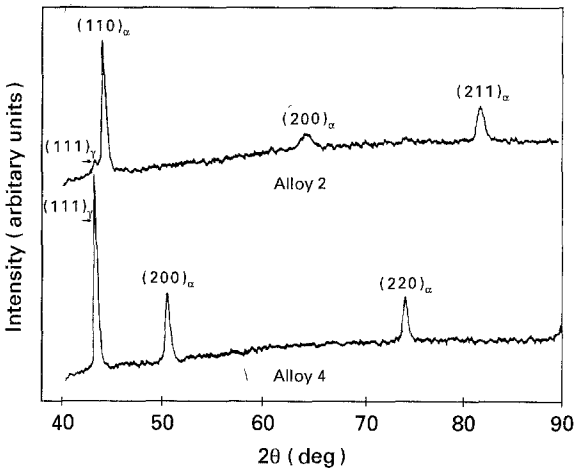

Figure 7 X-ray spectra obtained from the plastically deformed region of alloys 2 and 4: (α) martensite, (γ) austenite.

TABLE III Data obtained following tensile testing[a]

	Alloy 1		Alloy 2		Alloy 3		Alloy 4
	AN[b]	AN + LN[c]	AN	AN + LN	AN	AN + LN	AN
UTS, MPa	995	1120	780	1020	885.0	1110	705
% elongation, 32 mm GL[d]	31	25	43	27	33.0	14	23
% reduction in area	75	69	80	69	80.5	67	83
Transformed martensite, vol %	100	100	95	100	95.0	100	0
Hardness before test, H_V	210	360	160	325	200.0	310	180
Hardness after test, H_V	364	370	340	355	345.0	358	280

[a] All the values represent an average of three readings.
[b] AN, annealed sample.
[c] LN, liquid nitrogen quenched sample.
[d] GL, gauge length.

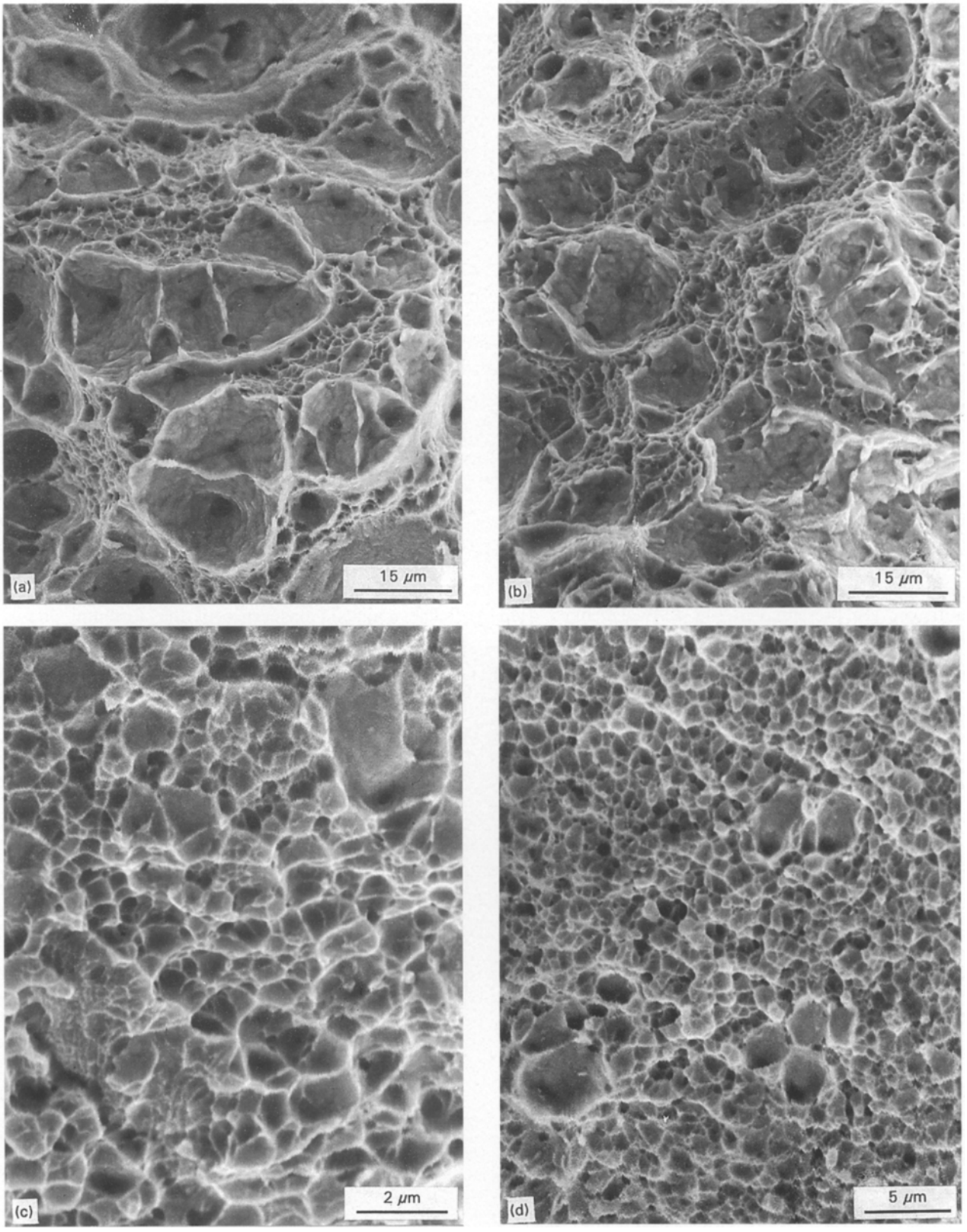

Figure 8 Fractographs obtained from alloy 3: (a) and (b) images from the primary fracture area, (c) and (d) image obtained from the shear lip area.

and following cold rolling of the annealed material. In contrast to the common belief that austenite is paramagnetic, the alloys investigated showed a different behaviour. The BH curves (Magnetic Hysterisis curve plotted between Saturation Magnetization ('B' units 'Tesla') and Coercive Field ('H' units Am^{-1})) obtained from annealed alloys 2, 3 and 4 are presented in Fig. 10 (the curve obtained from alloy 1 was quite similar to that of alloy 4 and therefore not included in the figure). The behaviour of alloys 1, 2 and 4 is typical of a material where domain alignment in the direction of the applied field is extremely different, i.e. typical of a material that is very weakly magnetic. However, unlike the paramagnetic material, hysterisis effect is present and coercivity measurable. The coercive field and saturation magnetization values of the alloys obtained under different treatments is presented in Table IV.

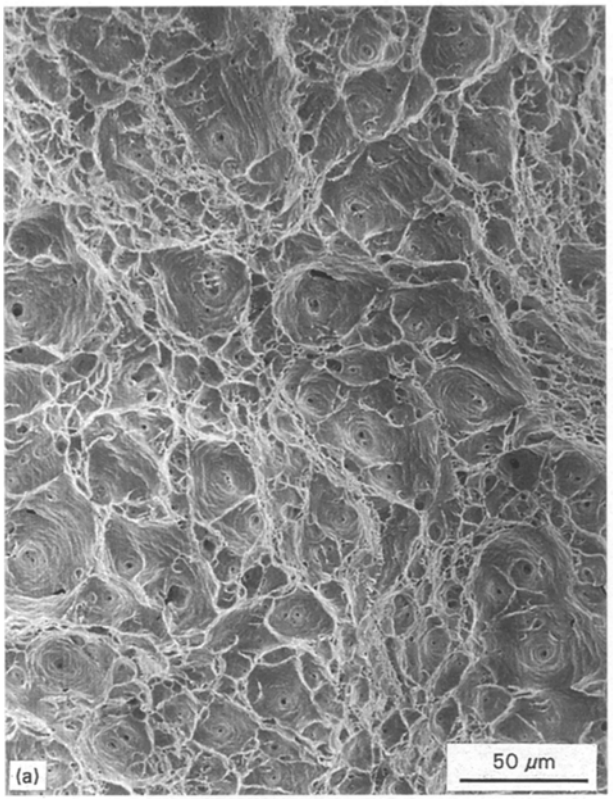

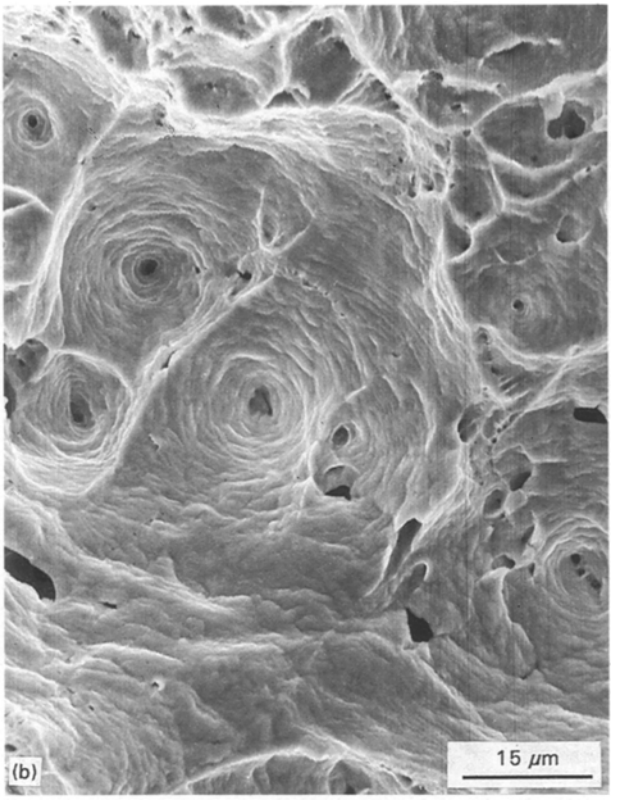

Figure 9 Fractographs obtained from alloy 4: (a) and (b) represent low and high magnification images from the primary fracture area, (c) image obtained from the shear lip region.

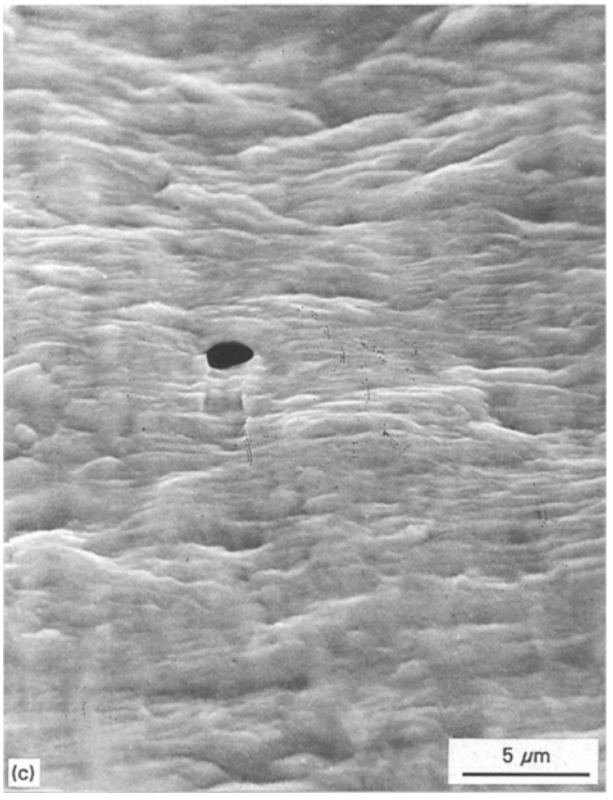

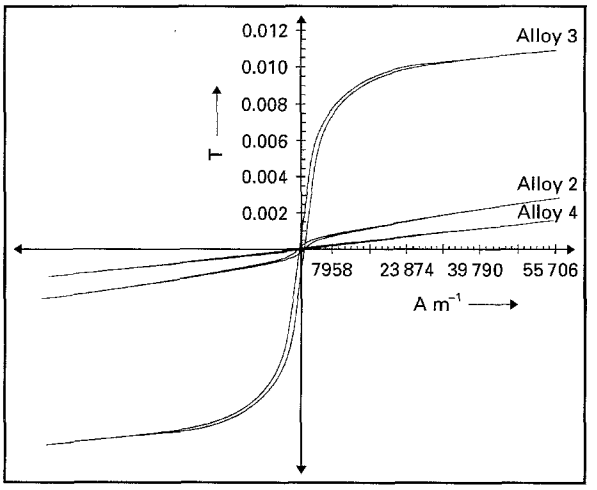

Figure 10 BH curve obtained from alloys 2, 3 and 4.

In contrast to the general behaviour, the response of alloy 3 to the applied field is that expected of a ferromagnetic material. The coercive field and saturation magnetization values were 1034 A m^{-1} and 11 T, respectively. The presence of ferromagnetic reverted austenite in combination with paramagnetic austenite in maraging steel has been suggested previously by Katz *et al.* [6]. However, in the present work, ferromagnetic austenite of known composition has been fabricated and its ferromagnetic behaviour clearly demonstrated.

The saturation magnetization values increased dramatically following dipping in liquid nitrogen. The only exception was alloy 4 where no change was observed. The increase was expected because of the transformation from the austenite to martensite phase. As alloy 4 remained austenitic, the values did not change. An increase in the coercive field was observed following martensitic transformation; the difference, however, was not as appreciable as seen in saturation magnetization. Further improvement in saturation magnetization could be incorporated,

TABLE IV Magnetic properties of the alloys

	Annealed		Annealed + liquid nitrogen quenched		Cold rolled	
	Am^{-1}	T	Am^{-1}	T	Am^{-1}	T
Alloy 1	2387	1.68	4774	14.70	2069	19.50
Alloy 2	1591	2.90	2546	16.30	1830	21.40
Alloy 3	1034	11.00	2546	18.70	1909	24.81
Alloy 4	2228	1.60	2228	1.60	2387	1.80

when the austenite phase was transformed into martensite by cold rolling. (Here also, the only exception was alloy 4 which remained austenitic regardless of the reduction ratio employed.) Higher values in saturation magnetization may be due to the fact that ~100% transformation to martensite occurs, while some retained austenite remains following dipping in liquid nitrogen. Texture incorporated during rolling is also known to improve saturation magnetization [2]. The coercive field in the as-rolled condition was similar to the annealed material. The relatively higher values observed following dipping in liquid nitrogen may be related to needle-like morphology of martensite that forms when liquid nitrogen treatment is applied.

4. Conclusions

1. The austenite phase remains stable up to ambient temperature when the concentration of Mo, Ni or Co is increased to 7.5, 24 and 25 wt %, respectively.

2. The Charpy impact strength of the austenitic alloys ranged between 260 and 294 J.

3. The austenite phases were found to be weakly magnetic. The only exception was the high Co containing alloy which exhibited ferromagnetic behaviour.

Acknowledgements

The authors would like to thank Dr Willayat Husain for his valuable comments and for his help in the preparation of alloys. We also thank T. N. Siddique for his help in X-ray analysis and M. Tahir and Afzal Hussain for their help in photography.

References

1. M. AHMED, I. NASIM and S. W. HUSAIN, *J. Mater. Engng & Performance*, **3(2)** (1994) 248.
2. M. AHMED, I. NASIM, I. SALAM, S. W. HUSAIN, F. H. HASHMI and A. Q. KHAN, *ibid.* **3** (1994) 386.
3. M. AHMED, A. ALI, S. K. HASNAIN, F. H. HASHMI and A. Q. KHAN, *Acta Metall. Mater.* **42** (1994) 631.
4. B. L. AVERBACK and M. COHEN, *Trans. AIME* **176** (1948) 401.
5. A. ALI, M. AHMED, F. H. HASHMI and A. Q. KHAN, *Mater. Sci. Technol.* **10** (1994) 97.
6. Y. KATZ, H. MATHIAS and S. NADIR, *Met. Trans.* **14A** (1983) 801.

Received 20 October 1994
and accepted 2 May 1995